Brief Report

Cell Stem Cell

Naive Human Pluripotent Cells Feature a Methylation Landscape Devoid of Blastocyst or Germline Memory

Graphical Abstract

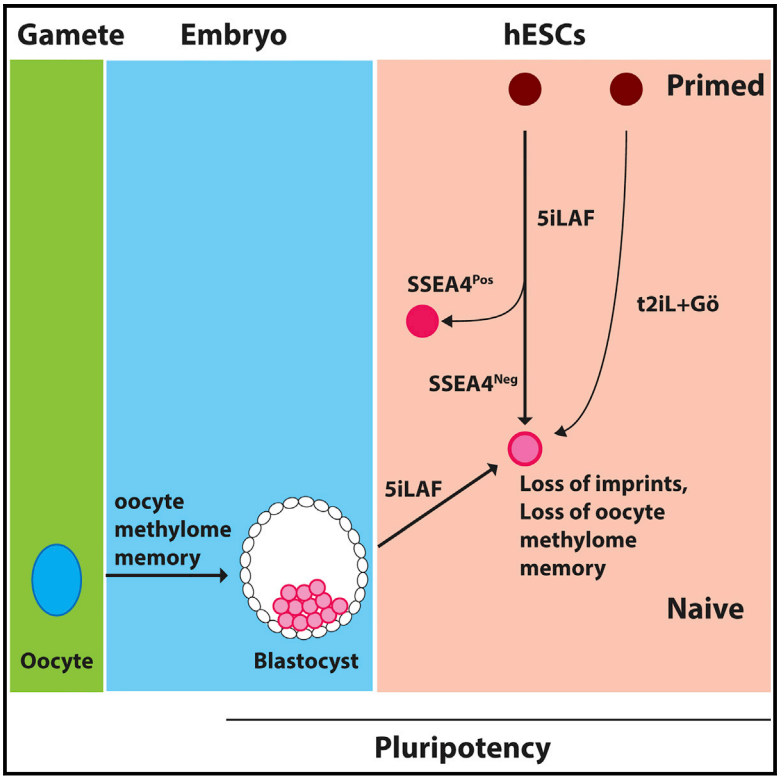

Authors

William A. Pastor, Di Chen, Wanlu Liu, ..., Kathrin Plath, Steven E. Jacobsen, Amander T. Clark

Correspondence

jacobsen@ucla.edu (S.E.J.), clarka@ucla.edu (A.T.C.)

In Brief

Pastor and colleagues show that reversion of primed hESCs in 5iLAF, or derivation of hESCs in 5iLAF, results in a population of naive cells characterized by loss of the marker SSEA4. However, these cells have a methylation pattern with little resemblance to blastocyst and near total loss of imprinting.

Highlights

- Reversion or derivation of hESCs in 5iLAF results in SSEA4-negative cells
- SSEA4-negative hESCs show gene expression consistent with naive pluripotency
- Naive hESCs show lost "memory" of gamete and blastocyst methylation
- Imprinting is lost in naive hESCs

Accession Numbers

GSE76970

Pastor et al., 2016, Cell Stem Cell *18*, 323–329
March 3, 2016
http://dx.doi.org/10.1016/j.stem.2016.01.019

Cell Stem Cell
Brief Report

Naive Human Pluripotent Cells Feature a Methylation Landscape Devoid of Blastocyst or Germline Memory

William A. Pastor,[1,5] Di Chen,[1,5] Wanlu Liu,[1,5] Rachel Kim,[3] Anna Sahakyan,[2] Anastasia Lukianchikov,[1] Kathrin Plath,[2,3] Steven E. Jacobsen,[1,2,3,4,*] and Amander T. Clark[1,3,*]
[1]Department of Molecular, Cell and Developmental Biology, University of California, Los Angeles, Los Angeles, CA 90095, USA
[2]Department of Biological Chemistry, University of California, Los Angeles, Los Angeles, CA 90095, USA
[3]Eli and Edythe Broad Center of Regenerative Medicine and Stem Cell Research, University of California, Los Angeles, Los Angeles, CA 90095, USA
[4]Howard Hughes Medical Institute, University of California, Los Angeles, Los Angeles, CA 90095, USA
[5]Co-first author
*Correspondence: jacobsen@ucla.edu (S.E.J.), clarka@ucla.edu (A.T.C.)
http://dx.doi.org/10.1016/j.stem.2016.01.019

SUMMARY

Human embryonic stem cells (hESCs) typically exhibit "primed" pluripotency, analogous to stem cells derived from the mouse post-implantation epiblast. This has led to a search for growth conditions that support self-renewal of hESCs akin to hypomethylated naive epiblast cells in human pre-implantation embryos. We have discovered that reverting primed hESCs to a hypomethylated naive state or deriving a new hESC line under naive conditions results in the establishment of Stage Specific Embryonic Antigen 4 (SSEA4)-negative hESC lines with a transcriptional program resembling the human pre-implantation epiblast. In contrast, we discovered that the methylome of naive hESCs in vitro is distinct from that of the human epiblast in vivo with loss of DNA methylation at primary imprints and a lost "memory" of the methylation state of the human oocyte. This failure to recover the naive epiblast methylation landscape appears to be a consistent feature of self-renewing hypomethylated naive hESCs in vitro.

Human embryonic stem cells (hESCs) are in vitro pluripotent cell types with the capacity for unlimited self-renewal and differentiation, making them critical models for understanding mechanisms required for human embryo development and differentiation. Although hESCs are derived from pre-implantation human blastocysts, they are morphologically and transcriptionally similar to murine epiblast stem cells (EpiSCs), which are derived from post-implantation mouse embryos. As such, hESCs and EpiSCs are said to exhibit a "primed pluripotent state" while mouse ESCs derived from the pre-implantation blastocyst exhibit a "naive pluripotent state" corresponding to an earlier stage of development (Nichols and Smith, 2009).

A number of culture conditions have recently been developed that promote maintenance and self-renewal of naive human pluripotent stem cells (Chan et al., 2013; Gafni et al., 2013; Takashima et al., 2014; Theunissen et al., 2014; Ware et al., 2014). Each protocol generates cell types with slightly different molecular characteristics, which may reflect metastable states in the spectrum of naive to primed pluripotency. A recent meta-analysis of sequencing data indicates that two of these protocols generate cells with a close transcriptional resemblance to the human pre-implantation epiblast (Huang et al., 2014). In the first protocol, hESCs are transfected with *KLF2* and *NANOG* and are cultured in media with titrated two inhibitors plus leukemia inhibitory factor and Gö6983 (t2iL+Gö) (Takashima et al., 2014). In the second protocol, primed cells can be reverted by being transferred to a media containing a cocktail of five inhibitors plus LIF, Activin, and/or Fibroblast Growth Factor 2 (5iLAF) (Theunissen et al., 2014). Using t2iL+Gö reversion of the H9 primed hESC line, it was shown that DNA methylation is globally reduced to the average level measured in human pre-implantation epiblasts (Takashima et al., 2014), with additional locus-specific erosion in the 5′ region of the LINE1 human specific (L1HS) retrotransposons (Gkountela et al., 2015). The DNA methylation profile of cells cultured in 5iLAF has never been evaluated.

Before studying the methylation pattern of 5iLAF cultured cells, we first wanted to confirm and characterize the naive phenotype. We performed n = 4 independent reversions of the hESC line UCLA1 (Diaz Perez et al., 2012) using 5iLAF (Theunissen et al., 2014). Upon the reversions we observed a mixture of small, round colonies similar to naive mESCs as well as flat, cobblestone-like colonies (Figures 1A and 1B). We evaluated one reversion using two classic human pluripotency surface markers called SSEA4 and TRA-1-81. Unlike primed UCLA1 hESCs, which are double positive for SSEA4 and TRA-1-81, the 5iLAF-reverted hESCs have a large fraction of double-negative cells (Figures 1A and 1B). Immunofluorescence staining showed that the SSEA4- and TRA-1-81-negative cells were still positive for OCT4 and NANOG (Figures S1A–S1F).

Next, we sorted the 5iLAF-cultured cells into SSEA4-positive and -negative populations using fluorescence-activated cell sorting (FACS) and re-plated the sorted cells onto MEFs in 5iLAF media (Figure 1C). We discovered that SSEA4-positive cells yielded mostly flat colonies, whereas SSEA4-negative cells

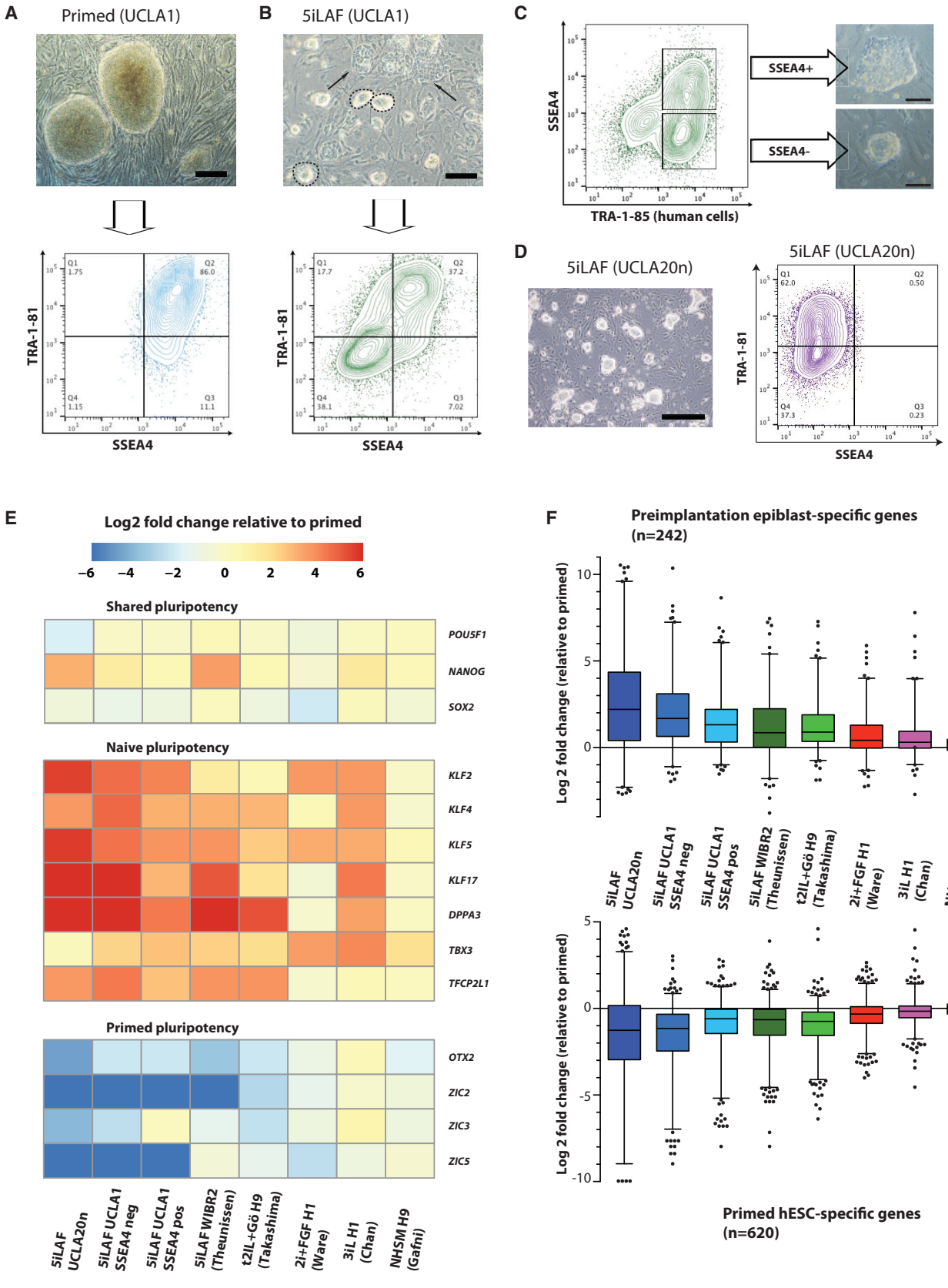

(legend on next page)

yielded mostly round colonies. One passage after sorting, the SSEA4-negative population remained SSEA4 negative, indicating that this is a relatively stable state (Figure S1G). We then reverted two additional lines called UCLA4 and UCLA5 (Diaz Perez et al., 2012) and found that small, round colony morphology was always enriched in the SSEA4-negative fraction whereas the SSEA4-positive cells yielded mostly flat, cobblestone colonies (Figures S1H–S1K).

In order to determine whether the heterogeneity in SSEA4 expression was also observed when deriving hESC lines completely under naive 5iLAF conditions, we derived n = 2 new hESC lines, which we have called UCLA19n and UCLA20n after thawing n = 7 day 5 vitrified human blastocysts. Colonies were uniformly round and flow cytometry revealed that UCLA19n was 85% SSEA4 negative (results not shown), whereas UCLA20n was almost completely SSEA4 negative (Figure 1D). In contrast, TRA-1-81 was expressed on a significant portion of SSEA4-negative cells in UCLA20n as well as reverted UCLA4 and UCLA5 hESC lines (Figure 1D, Figure S1I, Figure S1K). Therefore, loss of TRA-1-81 is not a consistent marker of naive morphology, whereas absence of SSEA4 is a highly correlated feature of naive round colony morphology. In summary, reversion of primed hESCs in 5iLAF generates a heterogeneous mixture of colonies, with SSEA4-negative hESCs correlating with small round colony morphology similar to naive hESCs derived from the human pre-implantation blastocyst.

On the basis of morphology, we speculated that 5iLAF SSEA4-negative hESCs are the naive population and thus transcriptionally resemble the cells of the human pre-implantation epiblast. To address this, we performed RNA-seq of 5iLAF-cultured SSEA4-positive or SSEA4-negative fractions of UCLA1, and we compared them to SSEA4-positive primed UCLA1 hESCs at equivalent passages (Table S1). We also performed RNA-seq of UCLA20n at passage 20 after derivation. We did not analyze UCLA19n as it was found to be 70% polyploid by passage 15. Consistent with the expression patterns of genes associated with naive pluripotency in mice, the 5iLAF SSEA4-negative cells and UCLA20n had elevated levels of *NANOG* as well as a dramatic upregulation of *KRUPPLE-LIKE FACTOR* (*KLF*) family transcription factors and reduced expression of primed state master regulators such as *ZINC FINGER OF THE CEREBELLUM* (*ZIC*) family transcription factors and *OTX2* (Buecker et al., 2014; Tang et al., 2011; Yang et al., 2014) (Figure 1E, Table S1). To further confirm the similarity of 5iLAF SSEA4-negative and UCLA20n hESCs to the human pre-implantation blastocyst, we used the previously published single-cell expression data from late pre-implantation epiblast and primed hESCs (Yan et al., 2013). We defined a set of "pre-implantation epiblast-specific" and "primed-specific" genes, which showed >4-fold difference in expression between these two cell types (Table S1). Using these genes as a reference, we found that the 5iLAF SSEA4-negative hESCs and UCLA20n had global upregulation of naive epiblast-specific genes and downregulation of primed-specific genes (Figure 1F).

In contrast, the SSEA4-positive hESCs sorted from 5iLAF cultures had an intermediate expression pattern between primed and naive, suggesting that SSEA4-positive cells that stably self-renew in 5iLAF are partially reverted to the naive state (Figures 1E and 1F). Comparing to published datasets, we found that the SSEA4-negative population in UCLA1 and the new hESC line UCLA20n is analogous to the original 5iLAF hESC lines created by reverting WIBR2 (Theunissen et al., 2014) and to t2iL+Gö-cultured hESCs created by reverting H9 (Takashima et al., 2014). In contrast, other published naive methods showed a less pronounced shift toward the naive state and failure to repress primed markers (Chan et al., 2013; Gafni et al., 2013; Ware et al., 2014). Interestingly, lines generated by these methods are also reported to be SSEA4 positive. Given these results, we focused our methylation analysis on the 5iLAF and t2iL+Gö conditions.

To determine the methylation pattern of hESCs in 5iLAF, we performed whole-genome bisulfite sequencing (WGBS) on two to four independent sorts of SSEA4-negative or SSEA4-positive reverted UCLA1 cells, SSEA4-negative UCLA20n cells, and primed UCLA1 cells that had been in culture a similar length of time to the reverted lines. We discovered that, similar to the levels observed in t2iL+Gö (Gkountela et al., 2015; Takashima et al., 2014), 5iLAF-cultured SSEA4-negative hESCs and UCLA20n had an average CG methylation level that resembled that of the human blastocyst (Figure 2A) (Okae et al., 2014).

In mammals the methylation pattern of the blastocyst is shaped by events during gametogenesis and early embryogenesis. The male pronucleus is selectively demethylated in early embryonic development, with only a few regions such as paternally methylated imprinted loci protected from DNA demethylation (Okae et al., 2014; Smith et al., 2012, 2014). Thus in humans the methylation pattern of the blastocyst strongly resembles that of the oocyte (Figures 2B and 2C). In contrast, the

Figure 1. 5iLAF SSEA4-Negative Subpopulation Recapitulates Naive Expression Pattern

(A) Upper: brightfield image of primed UCLA1 hESCs. Lower: flow cytometry plot of primed UCLA1 hESCs stained for SSEA4 and TRA-1-81. Scale bar indicates 200 μm.

(B) Upper: UCLA1 hESCs reverted in 5iLAF. A mixture of round (indicated with dotted circle) and flat colonies (indicated with arrow) are observed. Lower: flow cytometry plot of 5iLAF cultured UCLA1 hESCs stained for SSEA4 and TRA-1-81. Scale bar indicates 200 μm.

(C) 5iLAF cells were sorted into SSEA4-positive and SSEA4-negative populations. Upon re-plating, the SSEA4-positive cells formed flat colonies and the SSEA4-negative cells formed round colonies (n = 2 biological replicates). Scale bar indicates 100 μm.

(D) hESC line UCLA20n, derived from a 5-day human blastocyst in 5iLAF. Left: brightfield image. Scale bar indicates 200 μm. Right: flow cytometry plot of TRA-1-85^{+} (human) UCLA20n hESCs stained for SSEA4 and TRA-1-81.

(E) Expression of genes identified by others as associating with the naive and primed states in mice. Expression level is determined by RNA-seq. For 5iLAF SSEA4-negative (neg) and primed hESCs, n = 4. For 5iLAF SSEA4-positive (pos), n = 2. Other data comes from published RNA-seq or microarray datasets. Methodology, cell type, and citation are indicated.

(F) A set of "pre-implantation epiblast" and "primed" specific genes were defined based on published data. Expression of these genes is shown for various methodologies, relative to primed controls from the same dataset. UCLA20n was normalized to a primed UCLA1 library generated and sequenced at the same time.

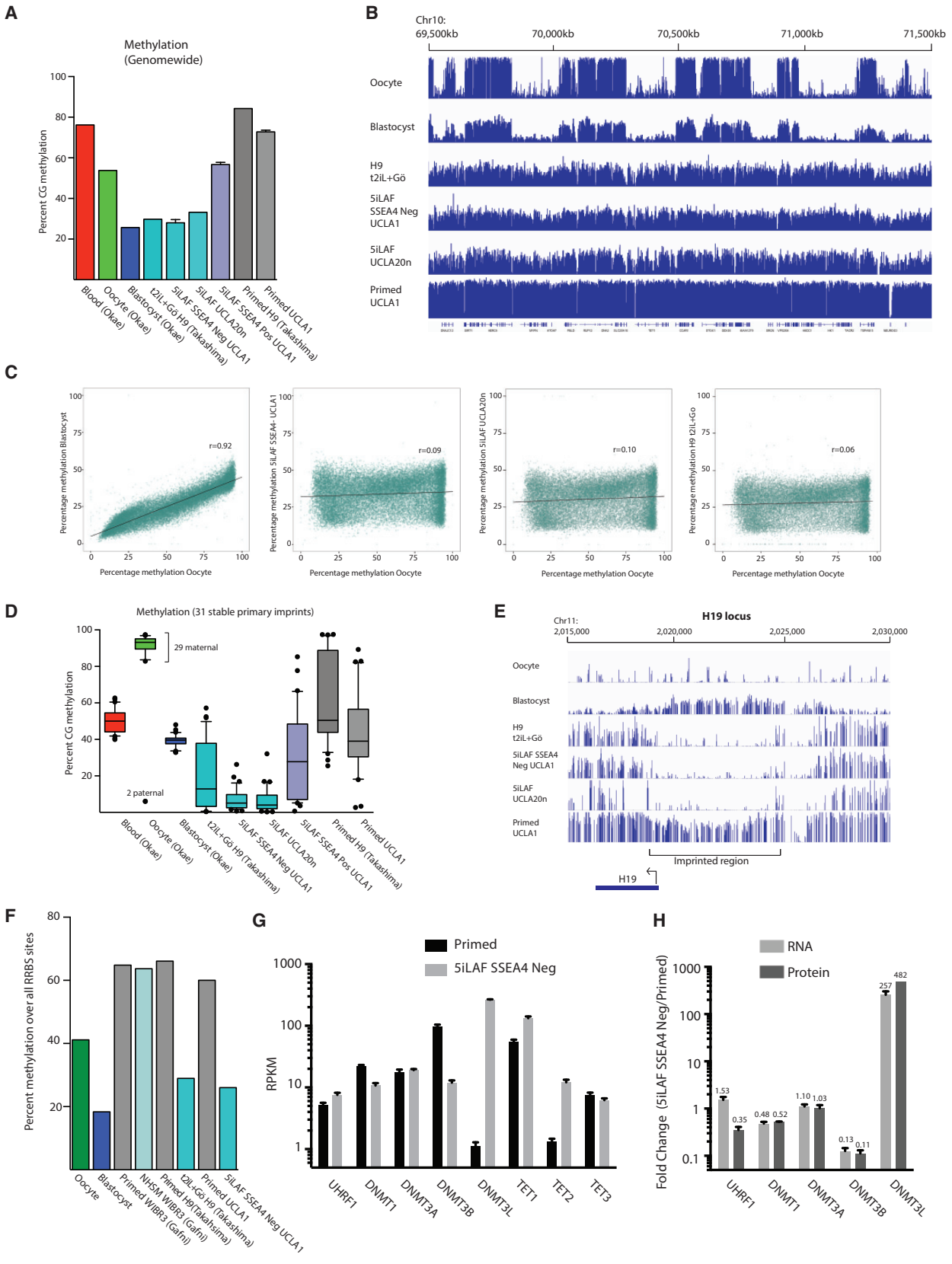

(legend on next page)

methylation landscapes of SSEA4-negative 5iLAF-cultured hESCs, UCLA20n, and t2iL+Gö-cultured cells are only weakly correlated with the human blastocyst and human oocyte (Figures 2B and 2C). Naive cells, even if cultured by different methodologies or derived directly from the human blastocyst, converge toward a methylation pattern that is different from that of the pre-implantation human blastocyst (Figures 2B and 2C). A striking example of this trend is observed at 332 CpG islands identified previously as ''transient maternal imprints:'' sites that are highly methylated in oocytes and the maternal chromosomes of blastocyst that lose methylation upon implantation (Smith et al., 2014). We discovered that reversion does not regenerate methylation at these sites, nor is methylation retained at these transient maternal imprints in the UCLA20n hESC line (Figure S2A).

An additional, striking deviation from oocyte and blastocyst methylation patterns in 5iLAF and t2iL+Go cultured cells occurred at stable imprints. These are regions where DNA methylation is established exclusively during germ-cell development. These methylated sites are protected from DNA demethylation during pre-implantation embryo development, remaining differentially methylated in somatic cells through the life of the organism and promoting a parent-of-origin-specific expression pattern in the neighboring genes. We examined DNA methylation at 29 maternally methylated stable primary imprints and 2 paternally methylated stable primary imprints (Okae et al., 2014) (Figure 2D, Table S2). There is roughly 50% methylation in somatic tissue and slightly below 50% methylation in blastocysts, as expected. In the primed UCLA1 hESCs used in our study, the median methylation of these imprinted sites was close to 50%, though some imprints were hyper- or hypomethylated, similar to what has been observed previously for other hESC lines (Rugg-Gunn et al., 2007). Strikingly, the 5iLAF SSEA4-negative hESCs and UCLA20n had near complete loss of methylation from all 31 primary stable imprints evaluated in our study, with loss over many imprints also found in t2iL+Gö (Figures 2D and 2E). Taking advantage of single nucleotide polymorphisms (SNPs) present in the UCLA1 hESC line, we observed a shift upon reversion in 5iLAF from monoallelic to biallelic expression of several imprinted genes including *H19* and *SNRPN*. (Figure S2B, Table S2). In order to determine whether methylation could be restored at imprinted genes by reverting the naive hESCs back to a primed state, we cultured 5iLAF SSEA4-negative and primed UCLA1 cells in primed epiblast-like cell (EpiLC) media (Hayashi et al., 2011) for 16 days. During this time, we discovered that 5iLAF SSEA4-negative cells showed a global shift toward expression of primed-specific genes and gained DNA methylation genome-wide (Figure S2C). However, increased methylation over imprinted regions was very modest, and biallelic expression was still observed (Figure S2D, Table S2). Thus, when lost, imprinting is not re-established in cells cultured in primed conditions, a similar scenario to the rescue of global DNA methylation, but not imprint methylation, in Dnmt1 knockout ESCs by the re-expression of Dnmt1 (Holm et al., 2005). Furthermore, consistent with data observed in hESCs cultured in t2iL+Gö (Gkountela et al., 2015), young LINE elements also show dramatic promoter hypomethylation in 5iLAF (Figure S2E).

Given the problem with maintenance of imprint methylation in naive cells, we considered the possibility that the 5iLAF SSEA4-positive cells may represent a useful intermediate. However, we discovered that the SSEA4-positive cells showed intermediate levels of global and imprint methylation loss (Figures 2C and 2D), with biallelic expression of *SNRPN* and *H19* (Table S2). We also analyzed the methylation loss imparted by naive human stem cell media (NHSM) (Gafni et al., 2013), which shows the smallest transcriptional shift toward naive pluripotency (Figures 1E and 1F). In order to directly compare our methylome data to findings of Gafni et al. (2013), we modified all whole-genome datasets to simulate the Reduced Representation Bisulfite Sequencing (RRBS) approach used by Gafni to measure DNA methylation. We discovered that imprint methylation was unperturbed in NHSM (Figure S2F), but very little global change in methylation was observed either (Figure 2F).

Consistent with an initial report of karyotypic instability in 5iLAF culture (Theunissen et al., 2014), we discovered that, 24 passages after reversion, the 5iLAF UCLA1 hESCs developed widespread karyotypic abnormalities, which was not observed in the first 13 passages following reversion (Figure S2G). Similarly, UCLA20n had evidence of trisomies at chromosomes 3, 7, 12, and 20 by passage 14 and as discussed above, UCLA19n was 70% polyploid at passage 15 (Figures S2G and S2H). Therefore, karyotypic instability may also be a frequent consequence of naive hESC culture.

To determine the cause of the cells' failure to maintain DNA methylation, we analyzed changes in RNA and protein levels of DNA methylation and demethylation machinery. We found that the RNA and protein levels of the de novo DNA methyltransferase DNMT3B dropped sharply in the 5iLAF SSEA4-negative cells,

Figure 2. Naive hESCs Fail to Recapitulate Naive-Specific Methylation Pattern

(A) Average genomewide-CG methylation level in primed and 5iLAF UCLA1 hESCs, shown in comparison with published datasets. For 5iLAF SSEA4-negative (neg) and primed hESCs, n = 3. For 5iLAF SSEA4-positive (pos), n = 2.

(B) DNA methylation is shown for a region of chromosome 10. Each bar indicates a single CG, and the height of the bar indicates the percentage of CG methylation. Where multiple CGs are too close to be visually rendered separately, an average value is shown.

(C) Correlation plots relative to human oocyte using 100 kb genome bins.

(D) DNA methylation over stable primary imprints. The average methylation level of each imprint in a given sample is represented as one point in the box and whisker point.

(E) DNA methylation over the paternally imprinted *H19* locus. Each bar indicates a single CG, and the height of the bar indicates the fraction of CG methylation. Where multiple CGs are too close to be visually rendered separately, an average value is shown.

(F) Total DNA methylation for three competing approaches for culturing naive cells. Because the Gafni et al. (2013) data was generated by RRBS, only CGs that had coverage in that dataset are included in this analysis to make the data comparable.

(G) Expression (RPKM) of DNA methyltransferases, DNMT cofactors, and Tet-family oxidases as measured by RNA-seq (n = 4).

(H) RNA and protein levels of DNA methyltransferases in 5iLAF SSEA4-neg UCLA1 hESCs relative to primed. RNA level is determined from RNA-seq data (n = 4) and protein level from quantitative westerns (UHRF1, n = 6 western blots; DNMT1, DNMT3A, and DNMT3B, n = 2; DNMT3L, n = 1).

while DNMT3A was unchanged and DNMT3L increased dramatically relative to primed hESCs. *UHRF1* RNA levels were slightly elevated in naive hESCs. However, at the protein level, we observed a 65% loss of UHRF1, and both *DNMT1* RNA and protein levels were reduced by 50% in the naive state. Furthermore, expression of the 5mC oxidases TET1 and TET2 increased substantially in the naive state (Figures 2G and 2H).

In the current study we have shown that naive hESCs have a transcriptional program enriched in human pre-implantation-specific genes but with a global DNA methylation landscape that is distinct from the normal state of the human pre-implantation blastocyst. The negative effect of the loss of ''transient imprints'' and the failure to recapitulate the oocyte-like methylation pattern is unclear. However, the loss of stable primary imprints is potentially serious in human pluripotent stem cell research. Correct imprinting is necessary for organism survival, and a number of rare human medical disorders have been linked to aberrant imprinting (Butler, 2009). Of note, murine embryonic germ cell lines are transcriptionally similar to murine ESCs but have widespread loss of imprints and contribute poorly to chimeras (Leitch et al., 2013; Oliveros-Etter et al., 2015; Tada et al., 1998), demonstrating the importance of imprints in correct differentiation of pluripotent cells in vivo. We also observed, in accompaniment to the loss of imprints, extensive karyotypic abnormalities in cells after their prolonged culture in 5iLAF. Loss of DNA methylation has been linked to karyotypic instability (Haaf, 1995).

We note that methylation at the imprinted loci is clearly depressed relative to that of surrounding regions. This may reflect the observation that many imprinted loci are promoters or regulatory elements that are active in the blastocyst (Rugg-Gunn et al., 2007). Thus if methylation is partially eroded at the imprint, the relevant transcription factors bind and cause further demethylation (as is generally the case at these genetic elements). In other words, methylation may be a very weak barrier to locus activation in 5iLAF. Similar dynamics may be at work at L1HS elements.

Although we observed a reduction in DNMT3B protein in the naive cells, we propose that this has only modest effects on creating the 5iLAF methylome given that *DNMT3A*$^{-/-}$ *DNMT3B*$^{-/-}$ DKO primed hESCs maintain primary imprints and show only modest DNA demethylation even after extended culture (Liao et al., 2015). We therefore propose that a combination of impaired maintenance methylation and increased TET activity could explain the majority of the 5iLAF hypomethylation phenotype. In a cell type with impaired maintenance and some continuous de novo methylation (imparted by DNMT3A and the remaining DNMT3B), DNA methylation levels will reach a steady state, but memory of previous methylation will be lost with DNA replication.

ACCESSION NUMBERS

The RNA-seq and BS-seq data in this paper are available under the GEO accession number GEO: GSE76970.

SUPPLEMENTAL INFORMATION

Supplemental Information for this article includes two figures, two tables, and Supplemental Experimental Procedures and can be found with this article online at http://dx.doi.org/10.1016/j.stem.2016.01.019.

AUTHOR CONTRIBUTIONS

The reversion and culture of hESCs in naive conditions was conducted by R.K., D.C., and A.S. hESC derivation from human blastocyst was undertaken by R.K. Experiments and data interpretation were conducted by D.C., W.A.P., A.L., and R.K. Computation analysis was conducted by W.L. and W.A.P. Conceiving and directing research were conducted by K.P., S.E.J., and A.T.C. Maintenance of University Compliance, including ESCRO, IRB, and Biological Safety, was overseen by A.T.C. The manuscript was written by W.A.P. and A.T.C.

ACKNOWLEDGMENTS

We thank the UCLA Broad Stem Cell Research Center (BSCRC) Flow Cytometry core for flow and FACS assistance, the UCLA BSCRC High Throughput Sequencing Core, Sriharsa Pradhan from N.E.B. for donating anti-DNMT1 antibody, and Steven Peckman from the UCLA BSCRC for consenting couples for embryo donation for hESC derivation. We thank Colin Shew, Beatrice Sun, and Tiasha Shafiq for help with experiments and the Fall 2015 UCLA Biomedical Research Minor 5HB undergraduate class for useful discussions. W.A.P. was supported by the Jane Coffin Childs Memorial Fund for Medical Research and a UCLA BSCRC Postdoctoral Training Fellowship. D.C. is supported by a UCLA BSCRC Postdoctoral Training Fellowship. W.L. is supported by the Philip J. Whitcome Fellowship from the UCLA Molecular Biology Institute and a scholarship from the Chinese Scholarship Council. This work was supported by the NIH R01 HD079546 (A.T.C.), CIRM RB4-06133 (K.P.), and P01 GM099134 (K.P.). Funds for human embryo banking and derivation of new hESC lines were provided by the UCLA Eli and Edythe Broad Center of Regenerative Medicine and Stem Cell Research. No federal grant funding was used for work with human embryo's or derivation of new hESC lines. No payment was provided to embryo donors for their generous gift of surplus embryos to stem cell research. S.E.J. is an investigator of the Howard Hughes Medical Institute.

Received: September 16, 2015
Revised: October 2, 2015
Accepted: January 15, 2016
Published: February 4, 2016

REFERENCES

Buecker, C., Srinivasan, R., Wu, Z., Calo, E., Acampora, D., Faial, T., Simeone, A., Tan, M., Swigut, T., and Wysocka, J. (2014). Reorganization of enhancer patterns in transition from naive to primed pluripotency. Cell Stem Cell *14*, 838–853.

Butler, M.G. (2009). Genomic imprinting disorders in humans: a mini-review. J. Assist. Reprod. Genet. *26*, 477–486.

Chan, Y.S., Göke, J., Ng, J.H., Lu, X., Gonzales, K.A., Tan, C.P., Tng, W.Q., Hong, Z.Z., Lim, Y.S., and Ng, H.H. (2013). Induction of a human pluripotent state with distinct regulatory circuitry that resembles preimplantation epiblast. Cell Stem Cell *13*, 663–675.

Diaz Perez, S.V., Kim, R., Li, Z., Marquez, V.E., Patel, S., Plath, K., and Clark, A.T. (2012). Derivation of new human embryonic stem cell lines reveals rapid epigenetic progression in vitro that can be prevented by chemical modification of chromatin. Hum. Mol. Genet. *21*, 751–764.

Gafni, O., Weinberger, L., Mansour, A.A., Manor, Y.S., Chomsky, E., Ben-Yosef, D., Kalma, Y., Viukov, S., Maza, I., Zviran, A., et al. (2013). Derivation of novel human ground state naive pluripotent stem cells. Nature *504*, 282–286.

Gkountela, S., Zhang, K.X., Shafiq, T.A., Liao, W.W., Hargan-Calvopiña, J., Chen, P.Y., and Clark, A.T. (2015). DNA Demethylation Dynamics in the Human Prenatal Germline. Cell *161*, 1425–1436.

Haaf, T. (1995). The effects of 5-azacytidine and 5-azadeoxycytidine on chromosome structure and function: implications for methylation-associated cellular processes. Pharmacol. Ther. *65*, 19–46.

Hayashi, K., Ohta, H., Kurimoto, K., Aramaki, S., and Saitou, M. (2011). Reconstitution of the mouse germ cell specification pathway in culture by pluripotent stem cells. Cell *146*, 519–532.

Holm, T.M., Jackson-Grusby, L., Brambrink, T., Yamada, Y., Rideout, W.M., 3rd, and Jaenisch, R. (2005). Global loss of imprinting leads to widespread tumorigenesis in adult mice. Cancer Cell *8*, 275–285.

Huang, K., Maruyama, T., and Fan, G. (2014). The naive state of human pluripotent stem cells: a synthesis of stem cell and preimplantation embryo transcriptome analyses. Cell Stem Cell *15*, 410–415.

Leitch, H.G., McEwen, K.R., Turp, A., Encheva, V., Carroll, T., Grabole, N., Mansfield, W., Nashun, B., Knezovich, J.G., Smith, A., et al. (2013). Naive pluripotency is associated with global DNA hypomethylation. Nat. Struct. Mol. Biol. *20*, 311–316.

Liao, J., Karnik, R., Gu, H., Ziller, M.J., Clement, K., Tsankov, A.M., Akopian, V., Gifford, C.A., Donaghey, J., Galonska, C., et al. (2015). Targeted disruption of DNMT1, DNMT3A and DNMT3B in human embryonic stem cells. Nat. Genet. *47*, 469–478.

Nichols, J., and Smith, A. (2009). Naive and primed pluripotent states. Cell Stem Cell *4*, 487–492.

Okae, H., Chiba, H., Hiura, H., Hamada, H., Sato, A., Utsunomiya, T., Kikuchi, H., Yoshida, H., Tanaka, A., Suyama, M., and Arima, T. (2014). Genome-wide analysis of DNA methylation dynamics during early human development. PLoS Genet. *10*, e1004868.

Oliveros-Etter, M., Li, Z., Nee, K., Hosohama, L., Hargan-Calvopina, J., Lee, S.A., Joti, P., Yu, J., and Clark, A.T. (2015). PGC Reversion to Pluripotency Involves Erasure of DNA Methylation from Imprinting Control Centers followed by Locus-Specific Re-methylation. Stem Cell Reports *5*, 337–349.

Rugg-Gunn, P.J., Ferguson-Smith, A.C., and Pedersen, R.A. (2007). Status of genomic imprinting in human embryonic stem cells as revealed by a large cohort of independently derived and maintained lines. Hum. Mol. Genet. *16* (Spec No. 2), R243–R251.

Smith, Z.D., Chan, M.M., Mikkelsen, T.S., Gu, H., Gnirke, A., Regev, A., and Meissner, A. (2012). A unique regulatory phase of DNA methylation in the early mammalian embryo. Nature *484*, 339–344.

Smith, Z.D., Chan, M.M., Humm, K.C., Karnik, R., Mekhoubad, S., Regev, A., Eggan, K., and Meissner, A. (2014). DNA methylation dynamics of the human preimplantation embryo. Nature *511*, 611–615.

Tada, T., Tada, M., Hilton, K., Barton, S.C., Sado, T., Takagi, N., and Surani, M.A. (1998). Epigenotype switching of imprintable loci in embryonic germ cells. Dev. Genes Evol. *207*, 551–561.

Takashima, Y., Guo, G., Loos, R., Nichols, J., Ficz, G., Krueger, F., Oxley, D., Santos, F., Clarke, J., Mansfield, W., et al. (2014). Resetting transcription factor control circuitry toward ground-state pluripotency in human. Cell *158*, 1254–1269.

Tang, F., Barbacioru, C., Nordman, E., Bao, S., Lee, C., Wang, X., Tuch, B.B., Heard, E., Lao, K., and Surani, M.A. (2011). Deterministic and stochastic allele specific gene expression in single mouse blastomeres. PLoS ONE *6*, e21208.

Theunissen, T.W., Powell, B.E., Wang, H., Mitalipova, M., Faddah, D.A., Reddy, J., Fan, Z.P., Maetzel, D., Ganz, K., Shi, L., et al. (2014). Systematic identification of culture conditions for induction and maintenance of naive human pluripotency. Cell Stem Cell *15*, 471–487.

Ware, C.B., Nelson, A.M., Mecham, B., Hesson, J., Zhou, W., Jonlin, E.C., Jimenez-Caliani, A.J., Deng, X., Cavanaugh, C., Cook, S., et al. (2014). Derivation of naive human embryonic stem cells. Proc. Natl. Acad. Sci. USA *111*, 4484–4489.

Yan, L., Yang, M., Guo, H., Yang, L., Wu, J., Li, R., Liu, P., Lian, Y., Zheng, X., Yan, J., et al. (2013). Single-cell RNA-Seq profiling of human preimplantation embryos and embryonic stem cells. Nat. Struct. Mol. Biol. *20*, 1131–1139.

Yang, S.H., Kalkan, T., Morissroe, C., Marks, H., Stunnenberg, H., Smith, A., and Sharrocks, A.D. (2014). Otx2 and Oct4 drive early enhancer activation during embryonic stem cell transition from naive pluripotency. Cell Rep. *7*, 1968–1981.